Liquid Crystals

ISSN: (Print) (Online) Journal homepage: https://www.tandfonline.com/loi/tlct20

Investigation of the mesogenic behavior of alkoxy and fluorine tail terminated alkoxy nitrobiphenyls for chemoresponsive liquid crystals

Mohammad S. Rahman, Trenton Wolter, Ayushi Tripathi, Nicholas L. Abbott, Manos Mavrikakis & Robert J. Twieg

To cite this article: Mohammad S. Rahman, Trenton Wolter, Ayushi Tripathi, Nicholas L. Abbott, Manos Mavrikakis & Robert J. Twieg (2022): Investigation of the mesogenic behavior of alkoxy and fluorine tail terminated alkoxy nitrobiphenyls for chemoresponsive liquid crystals, Liquid Crystals, DOI: 10.1080/02678292.2022.2103193

To link to this article: https://doi.org/10.1080/02678292.2022.2103193

Published online: 05 Aug 2022.

LIQUID CRYSTALS
https://doi.org/10.1080/02678292.2022.2103193

Taylor & Francis
Taylor & Francis Group

Investigation of the mesogenic behavior of alkoxy and fluorine tail terminated alkoxy nitrobiphenyls for chemoresponsive liquid crystals

Mohammad S. Rahman[a], Trenton Wolter[b], Ayushi Tripathi[c], Nicholas L. Abbott[c], Manos Mavrikakis[b] and Robert J. Twieg[a]

[a]Department of Chemistry and Biochemistry, Kent State University, Kent, OH, USA; [b]Department of Chemical and Biological Engineering, University of Wisconsin-Madison, Madison, WI, USA; [c]Department of Chemical and Biomolecular Engineering, Cornell University, Ithaca, NY, USA

ABSTRACT

Liquid crystal properties of compounds with a variety of polar terminal groups including cyano, fluoro, isothiocyanato, etc., were studied well, however, not enough attention was given to nitro terminal compounds. In this work, a series of fluorine tail terminated alkoxy nitrobiphenyl compounds were synthesised and their mesogenic properties were analysed. In addition, the simple alkoxy nitrobiphenyl compounds were synthesised and analysed in order to compare them with fluoro-alkoxy nitrobiphenyl compounds and for binary mixture analysis. Fluorine tail termination to the alkoxy chain does suppress the smectic phase that was observed for the simple alkoxy nitrobiphenyl compounds with longer chains. Fluorine tail terminated alkoxy nitrobiphenyl compounds with longer chains (C7-C10) show monotropic nematic phase around ambient temperature and supercooling properties and these compounds are useful for a binary mixture analysis. Moreover, computation and experimental analyses of the alkoxy nitrobiphenyl compounds were performed to investigate the potential use of these nitro terminal compounds as chemoresponsive liquid crystal materials.

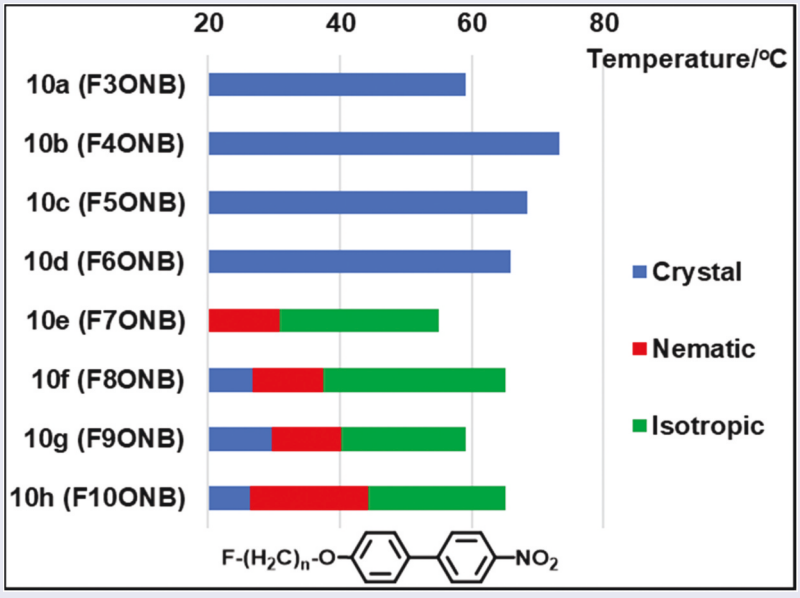

ARTICLE HISTORY
Received 6 June 2022
Accepted 14 July 2022

KEYWORDS
Nitrobiphenyl; tail fluorinated alkoxy; nucleophilic substitution reaction (S_N2); nematic phase; homeotropic anchoring; chemoresponsive sensor

1. Introduction

Liquid crystal (LC) compounds have been widely used as responsive materials in a range of technologies, especially in the universal LC display [1]. Significant effort persists to further enhance display performance of nematic displays and other technologies are being pursued as well. Besides LC displays, liquid crystals are being used to develop chemoresponsive liquid crystal (LC) sensors which can be used widely to detect the presence of atmospheric pollutants (ozone, sulphur dioxide etc.), chemical

CONTACT Manos Mavrikakis emavrikakis@wisc.edu; Robert J. Twieg rtwieg@kent.edu

warfare agents (sarin), and other vapour-phase toxins (Cl_2, NO_2 etc.) at concentrations in the low ppm range [2–4]. The important feature of an effective LC sensor is that it must be activated rapidly and selectively in the presence of target analytes. Chemoresponsive LC sensors comprise a nematic LC (a type of LC) film deposited on a reactive substrate that undergoes a detectable change in its adsorption, orientation, and optical properties when exposed to a vapour stream containing the analyte [2]. Therefore, exploitation of such chemoresponsive sensors depends on the availability of suitable nematic liquid crystal compounds.

Liquid crystals with broad ambient nematic phases have attracted tremendous interest because of their potential applications in the display devices such as laptop, cell phone, smart watch, etc. [1,5–7]. To develop such liquid crystals, extensive studies have been performed by many research groups to elucidate the structure-property relationships of the mesogenic materials. This can be achieved via subtle changes to the molecular structure in a variety of ways as shown in Figure 1 for simple rod-like (calamitic) biphenyl core compounds. For example, as in the case of a biphenyl core system, the mesogenic property of liquid crystal compounds can be tuned via (i) changing the polar terminal **X** group (CN, NCS, NO_2, etc.); (ii) modification of the flexible chain **R** by incorporation of single atom or bulky group **Z** at the end of the chain or by other means; and/or (iii) modifying the rigid aromatic core **A**-**B** by lateral substitution of **Y**.

To date, many alkyl (K series) and alkoxy (M series) biphenyl liquid crystal compounds incorporating a polar terminal **X** group (CN, F, NCS, etc.) have been developed. Amongst the many liquid crystal compounds, 4-*n*-pentyl-4'-cyanobiphenyl (5CB) is especially well known due to its favourable room temperature nematic phase property [5]. The Itahara group also reported other promising liquid crystal compounds comprising alkoxy cyanobiphenyls with pentafluorophenyloxy tail termination, which show nematic phase properties close to ambient temperature [8].

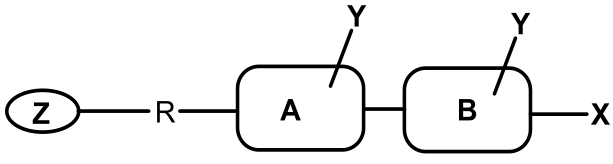

Figure 1. A general structure for a biphenyl core calamitic liquid crystal (where **X** = polar terminal group; **Y** = H or lateral group; **R** = alkyl or alkoxy chain; **Z** = H or single atom or bulky group; **A-B** = benzene rings comprising the biphenyl).

Therefore, the search for room temperature nematic liquid crystal compounds with enhanced mesogenic properties required for practical applications has never stopped. Recently, our group has developed many K and M series cyanobiphenyl (CB) derivatives using a variety of terminal **Z** functionalised flexible chains. These **Z** groups include cyano [9], hydroxy [10], fluoro [11], aryl and aryloxy [12] termini on alkyl and alkoxy CBs. In addition, a number of liquid crystal compounds with other terminally Z functionalised flexible chains have been reported by other research groups that include bromo [13–15], chloro [13,14], thiol [16] and olefin [17] terminated alkoxy cyanobiphenyls. The terminal functionalization of the flexible chain has shown some promise in improving mesogenic properties of liquid crystal compounds. For example – incorporation of single fluorine atom or a thiol functional group in lieu of hydrogen atom at the end of the flexible chain can destabilise the smectic phase that is typically observed for both the K and M series of cyanobiphenyl derivatives with longer chains [11]. The hydroxy tail terminated K and M series of cyanobiphenyls sometimes exhibit stable nematic phase property at higher temperature compared to the simple K and M series of cyanobiphenyls [10]. It has also been demonstrated previously for some compounds that substitution of a single hydrogen atom by a halogen atom (F, Cl and Br), or bulky groups (-OH, -SH) at the chain terminus can significantly reduce the K-N transition temperature with only minimal change in the *N*-I transition temperature [11]. In addition, our group has reported that some rigid core fluorinated alkoxy CBs with perfluoro phenoxy tail termination have shown promising results in exhibiting nematic phase property at and below room temperature as individual compounds and as mixtures [12].

Many alkyl (K type) and alkoxy (M type) cyanobiphenyl compounds are known. However, it is surprising to see that much less is known about the respective polar nitro (-NO_2) terminal alkyl and alkoxy biphenyl compounds. Only a single alkyl nitrobiphenyl (4-*n*-heptyl-4'-nitrobiphenyl, 7NB) has been reported while a series of simple hydrogen tail terminated 4-alkoxy-4'-nitrobiphenyl (nONB, $n = 3–11$) compounds were previously synthesised and their mesogenic properties investigated [18–20]. In this work, we report the synthesis of a novel series of fluorine tail terminated 4-alkoxy-4'-nitrobiphenyl compounds and lateral fluorine substituted 4-alkoxy-4'-nitrobiphenyl compounds. Here, the independent synthesis of a series of simple hydrogen tail terminated 4-alkoxy-4'-nitrobiphenyl using a literature procedure is also reported [21]. The phase behaviour of the fluorine and simple hydrogen tail terminated, and lateral fluorine substituted, 4-alkoxy-4'-nitrobiphenyl

analogs was investigated and their mesophase behaviours are compared. Just as in the case of the cyanobiphenyls, this study of nitrobiphenyls is motivated by their potential application in sensor applications.

2. Experimental section

2.1. Synthesis

The target 4-alkoxy-4'-nitrobiphenyls **5a-g** (nONB) and fluorine tail terminated 4-alkoxy-4'-nitrobiphenyls **10a-g** (FnONB) have been synthesised from the starting material 4-hydroxy-4'-nitrobiphenyl **4** as shown in Schemes 1 and 2 respectively. The 4-hydroxy-4'-nitrobiphenyl **4** was synthesised according to the literature procedure from commercially available 4-biphenol [18,22]. In this process the hydroxy group of 4-biphenol was protected by reacting with benzoyl chloride in the presence triethylamine to generate biphenyl-4-yl benzoate **2**. The nitration of compound **2** using concentrated nitric acid in the presence of sodium nitrite produced 4-nitrobiphenyl-4'-yl benzoate **3** as a major product along with 2-nitrobiphenyl-4'-yl benzoate as a minor product. The minor byproduct was separated during the recrystallisation process. Finally, deprotection of the ester group under basic conditions leads to the formation of the important phenolic precursor 4-hydroxy-4'-nitrobiphenyl **4**. Next, alkylation of **4** with respective alkyl halides using K_2CO_3 as a base via S_N2 reaction process leads to the formation of desired 4-alkoxy-4'-nitrobiphenyls (**5a-g**) [21].

The corresponding set of fluorine tail terminated 4-alkoxy-4'-nitrobiphenyls **10a-h** (**FONBs**) were synthesised from 4-hydroxy-4'-nitrobiphenyl by a variety of routes as summarised in Scheme 2. In the case of compound **10a** ($n = 3$, F3ONB) the 4-hydroxy-4'-nitrobiphenyl was alkylated under Mitsunobu reaction conditions using commercially available 3-fluoropropanol and diisopropyl azodicarboxylate (DIAD). The compounds **10b** ($n = 4$, F4ONB), **10c** ($n = 5$, F5ONB), **10f** ($n = 8$, F8ONB), **10 g** ($n = 9$, F9ONB) and **10 h** ($n = 10$, F10ONB) were all prepared by direct alkylation of 4-hydroxy-4'-nitrobiphenyl via S_N2 reaction using commercially available 1-bromo-4-fluorobutane and 1-bromo-5-fluoropentane and synthesised 1-chloro-8-fluorooctane and 1-bromo-9-fluorononane, respectively. Compounds **10d** ($n = 6$, F6ONB) and **10e** ($n = 7$, F7ONB) were synthesised via multistep reaction processes. Here alkylation of 4-hydroxy-4'-nitrobiphenyl via S_N2 reaction process using respective hydroxy tail alkyl halides generated hydroxy tail alkoxy biphenyls **6** ($n = 6$) and **8** ($n = 7$). Next, tosylation of hydroxy tail compounds **6** and **8** using

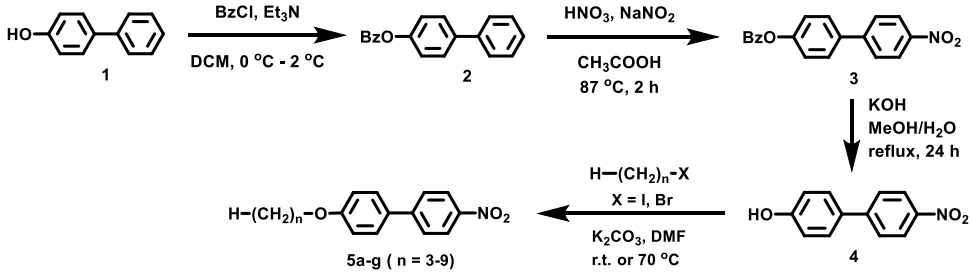

Scheme 1. Synthetic pathways for the 4-alkoxy-4′-nitrobiphenyls **5a-g** (nONB).

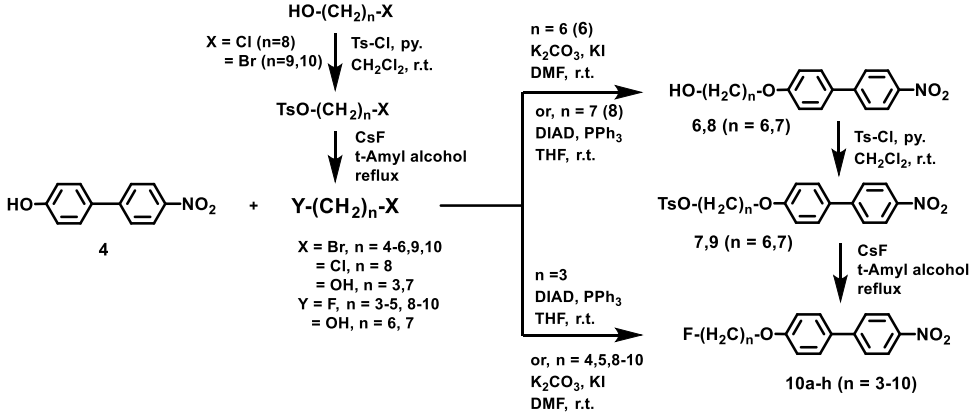

Scheme 2. Synthetic pathways utilized for preparation of the fluorine tail terminated 4-alkoxy-4′-nitrobiphenyls (**10a-h**).

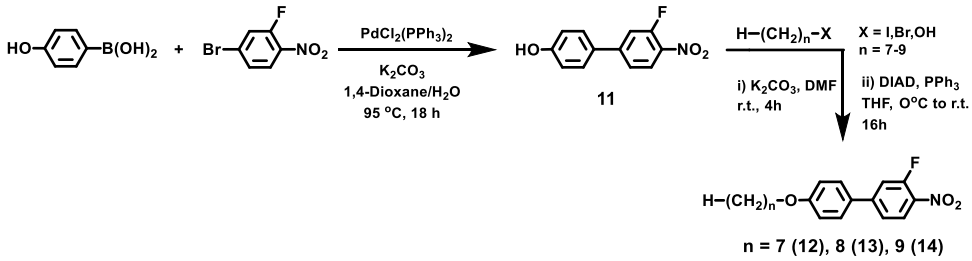

Scheme 3. Synthetic pathways employed for the synthesis of the lateral fluorinated 4-alkoxy-4′-nitrobiphenyls **12-14**.

p-toluenesulfonyl chloride in the presence of pyridine produced the tosylated alkoxy nitrobiphenyls **7** ($n = 6$) and **9** ($n = 7$) [23]. Finally, nucleophilic fluorination of these tosylated alkoxy nitrobiphenyls **7** and **9** using caesium fluoride afforded the desired compounds **10d** and **10e**. It was found that direct tosylation of hydroxy-tail terminated nitrobiphenyls (**7** and **9**) was incomplete over a longer time and was a low yielding reaction step. Therefore, the fluorine-tail substituted alkyl halides 8-chloro-1-fluorooctane and 9-bromo-1-fluorononane were synthesised in two steps from the commercially available hydroxy tail alkyl halides according to the literature adapted procedures in order to synthesise fluorine tail alkoxy nitrobiphenyls [11,24]. First, tosylation of alcohols were performed using *p*-toluenesulfonyl chloride in the presence of pyridine and second, nucleophilic fluorination of tosylated alkyl halides using caesium fluoride under reflux condition generated 1-chloro-8-fluorooctane and 1-bromo-9-fluorononane. Of course, the synthesis routes actually utilised in this study for compounds **10a-h** are not unique and the different approaches discussed should apply to most of them.

The synthesis of aromatic core fluorinated 4-alkoxy-4'-nitrobiphenyl compounds **12-14** (nONBF) is shown in Scheme 3. The important precursor 4-hydroxy-3'-fluoro-4'-nitrobiphenyl was prepared via Suzuki coupling reaction between 4-hydroxyphenylboronic acid and 4-bromo-2-fluoronitrobenzene using dichlorobis-(triphenylphosphine)palladium (II) as catalyst. Next, the alkylated target compounds **12-14** were prepared in two reaction pathways based on the availability of the specific relevant starting material. Compound **12** ($n = 7$) and **14** ($n = 9$) was prepared via S_N2 reaction pathway from the precursor **11** and corresponding alkyl halide using potassium carbonate as a base. Compound **13** was prepared via Mitsunobu reaction conditions from the precursor **11** and 1-octanol using diisopropyl azodicarboxylate (DIAD). All the synthesised compounds were characterised by ^{1}H and ^{13}C NMR spectroscopy and in some case ^{19}F NMR and high-resolution mass spectrometry as well.

2.2. Computational methods

All density functional theory (DFT) calculations were performed using Gaussian 09 [25]. For dipole moment calculations, geometry optimisation calculations were performed at the PBE-D3(SMD = benzonitrile)/def2-SVP level of theory [26–29]. Electronic energies were obtained from a subsequent single-point calculation at the M06-2X-D3(SMD = benzonitrile)/def2-TZVP level of theory [30] while free energy contributions were obtained from the PBE-D3(SMD = benzonitrile)/def2-SVP level of theory. Each dihedral angle in the molecule tail was evaluated at 60-, 180-, and 300-degree angles. Because there are three possible angles for each C-C or C-O bond in the alkoxy tail, the number of possible configurations for each tail length was 3^n, where n is the number of carbon atoms in the tail. To maintain computational efficiency, all configurations were accounted for for n less than 7, and 1500 configurations were randomly sampled for $n \geq 7$. Boltzmann weights were calculated at room temperature and used to obtain an average dipole moment for each molecule. This method of calculating the dipole moment has been successfully used in the past [9–12].

Gibbs free binding energies were calculated using the Neutral Anion Model (NAM) that has been discussed in past publications [4,31,32] to help understand the anchoring behaviour of liquid crystals on metal-salt surfaces. Binding free energies were calculated using the following equation:

$$G_{BE} = G_{tot} - G_{NAM} - G_{ads}$$

where G_{BE} is the Gibbs free binding energy and G_{tot}, G_{NAM}, and G_{ads} are the Gibbs free energies of the final adsorbed state (NAM+adsorbate), the NAM alone, and the adsorbate alone, respectively. For these calculations, geometry optimisations were performed at the PBE-D3/def2-SVP level of theory, and total energies were obtained from a subsequent single-point calculation at the M06-2X-D3/def2-TZVP level of theory. Free energy contributions were calculated at the PBE-D3/def2-SVP level of theory with a temperature of 310 K.

Displacement free energies for DMMP displacing a liquid crystal molecule were calculated using the following equation:

$$G_{DE} = G_{BE,DMMP} - G_{BE,LC}$$

where G_{DE} is the displacement free energy, $G_{BE,DMMP}$ is the binding free energy of DMMP on the metal salt (NAM model), and $G_{BE,LC}$ is the binding free energy of the liquid crystal molecule on the metal salt (NAM model).

2.3. Results and discussion

The mesogenic behaviour and the transition temperatures of the 4-alkoxy-4'-nitrobiphenyls **5a-g** (nONB) and the analogous fluorine tail terminated 4-alkoxy-4'-nitrobiphenyls **10a-h** (FnONB) were investigated by both Differential Scanning Calorimetry (DSC) and Polarised Optical Microscopy (POM). The POM data is summarised in Table 1. The phase behaviour of the previously reported non-fluorine tail terminated 4-alkoxy-4'-nitrobiphenyls is also included for comparison.

The alkoxy nitrobiphenyl series **5a-g** ($n = 3$–9) with conventional all hydrogen tail termination is summarised in Chart 1 and will be discussed first. The phase behaviour of the alkoxy nitrobiphenyl series **5a-d** and **5 g** ($n = 3$–6 and 9) exactly matches with the literature reported values but differs for the (7ONB) and (8ONB) compounds **5e** and **5f**. It was observed for carbon chains $n = 3$–5 the alkoxy nitrobiphenyls 3ONB (**5a**), 4ONB (**5b**) and 5ONB (**5c**) did not exhibit any mesophase properties but all showed supercooling properties For the six carbon chain alkoxy nitrobiphenyl 6ONB (**5d**), no mesophase transition was observed by DSC analysis, however, a narrow monotropic nematic phase transition was observed by POM analysis (see Figure SI), which is in agreement with the literature report [18]. For the seven carbon chain alkoxy nitrobiphenyl 7ONB (**5e**), it was reported in the literature that **5e** showed monotropic nematic and smectic phase properties close to room temperature. However, in our experiments, DSC **5e** exhibits a monotropic nematic phase transition at 48.2°C along with a weaker transition at 33.2°C assumed to be a smectic phase transition based on POM analysis. In contrast, POM analysis of **5e** shows a narrow enantiotropic nematic phase property and supercooling. It is also noted that during POM analysis of **5e**, on cooling a clear smectic phase was observed at 32.6°C (see Chart 1) which agrees with literature reported analysis. The phase behaviour of the alkoxy nitrobiphenyl **5f** with an eight-carbon chain was reported in the literature where both stable smectic and nematic phase transitions were observed. However, in our experiments **5f** exhibits a stable nematic but no stable smectic phase transition. Moreover, on cooling an unknown biphasic (i.e. both isotropic and liquid crystal) transition was observed at 46.3°C besides nematic phase transition at 49°C (see Chart 1). Further experiments are ongoing to elucidate this phase transition. The nine-carbon chain shows only a smectic phase transition at 53.3°C (see SI). This behaviour of **5 g** agrees with the well-known tendency towards smectic phase transitions as the length of the carbon chain increases.

Previously, our group reported that terminal tail fluorination in 4-ω-fluoroalkoxy-4'-cyanobiphenyls (FnOCB) generally reduced the K-N transition temperature and that these compounds exhibited larger supercooling properties compared to 4-alkoxy-4'-cyanobiphenyls (nOCB) [11]. In addition, terminal tail fluorination of 4-alkoxy-4'-cyanobiphenyls (for 8OCB and 9OCB) was found to often eliminate the smectic phase and thus facilitate nematic phase formation [11].

Table 1. Phase behaviour data of the 4-alkoxy-4′-nitrobiphenyls 5a-g (nOnb) [19]. And the corresponding fluorine tail terminated 4-alkoxy-4′-nitrobiphenyls 10a-h (FnONB) determined by POM.

n	nONB	$H(H_2C)_n$–O–⟨⟩–⟨⟩–NO_2	FnONB	$F(H_2C)_n$–O–⟨⟩–⟨⟩–NO_2
3	5a (3ONB)	K 73.6 I 59.8 K Literature: K 74.1 I	10a (F3ONB)	K 59.1 I 43.4 K
4	5b (4ONB)	K 79.8 I 66.6 K Lit.: K 80.6 I	10b (F4ONB)	K 73.4 I 41.1 K
5	5c (5ONB)	K 53.7 I 40.9 K Lit.: K 54.7 I	10c (F5ONB)	K 68.5 I 37.2 K
6	5d (6ONB)	K 65.7 I 34.5 N 29.7 K Lit.: K 67.6 I	10d (F6ONB)	K 65.9 I
7	5e (7ONB)	K 36.3 N 39.1 I 38.9 N 32.6 Sm Lit.: K 36.5 (Sm 30.5) (N 38.5) I	10e (F7ONB)	K 52.2 I 28.1 N
8	5f (8ONB)	K 48.5 N 49.6 I 49 N 46.3 (Sm?) 33.3 K Lit.: K 49.2 Sm 50.2 N 52.2 I	10f (F8ONB)	K 65.2 I 37.4 N 26.8 K
9	5g (9ONB)	K 57.4 I 53.3 Sm 30.4 K1 27.4 K2 Lit.: K 56.5 Sm 56.7 I	10g (F9ONB)	K 59 I 40.1 N 29.7 K
10	5h (10ONB)	Lit.: K 70.3 (68.3 Sm) I	10h (F10ONB)	K 65.1 I 44.3 N 26.3 K

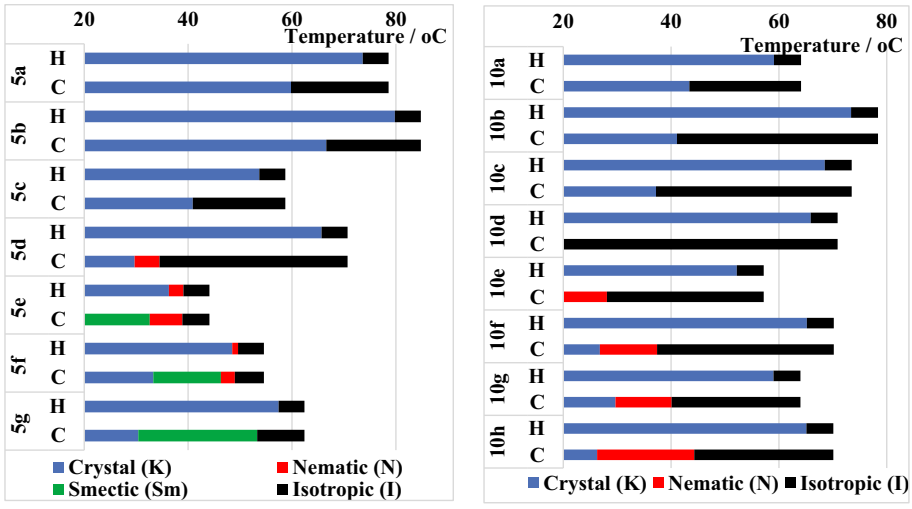

(a) (b)

Chart 1. (Colour online) The thermal behavior of (a) hydrogen tail terminated 4-alkoxy-4′-nitrobiphenyls **5a-g** (nONB) and (b) fluorine tail terminated 4-alkoxy-4′-nitrobiphenyls **10a-h** (FnONB). Compounds 3ONB, 4ONB, 5ONB, F3ONB, F4ONB F5ONB and F6ONB are not mesogenic. Heating cycles are shown for enantiotropic nematogens 7ONB and 8ONB. Only the cooling cycles of 6ONB, 9ONB, F7ONB, F8ONB and F9ONB are shown since they show mesogenic behavior only upon cooling (Figure 2).

Therefore, to investigate the effect of terminal fluorination of the alkyl chain, a series of fluorine tail terminated 4-alkoxy-4'-nitrobiphenyls **10a-g** (n = 3–9, FnONB) are developed and compared. It was observed for carbon chains n = 3–6 the fluorine tail terminated alkoxy nitrobiphenyls **10a-d** (F3ONB, F4ONB and F5ONB) did not exhibit any mesophase properties, but all showed significant supercooling properties. For carbon chains n = 7–9 (**10e-h**; F7ONB, F8ONB, F9ONB and F10NB) monotropic nematic behaviour was found for all of these compounds. No smectic phases were observed in the entire **10a-h** series.

The introduction of a single fluorine atom at the end of the alkyl tail modifies the mesogenic behaviour in several ways. For n = 3–5, there was no mesogenic behaviour found in either the nonfluorinated or fluorinated compounds. At n = 6 the series begin to differ as there is a monotropic nematic phase for **5d** (6ONB) and no mesophase for **10d** (F6ONB). At n = 7–9 smectic phases appear in the nonfluorinated compounds 7ONB, 8ONB, 9ONB and 10ONB (and nematic behaviour disappears at n = 9–10) while there are no smectic phases at all found in the analogous fluorine terminated compounds F7ONB, F8ONB, F9ONB and F10NB. So, one of the main influences of fluorine tail termination is to suppress the smectic phase (as previously observed in the analogous series of cyanobiphenyls (FnOCB)) [11]. Upon cooling, compound **10e** (F7ONB) recrystallises at −2.8°C shown by DSC analysis after exhibiting a wide nematic range below room temperature. In addition, the mesophase behaviour of the analogous hydroxy tail terminated 4-alkoxy-4'-nitrobiphenyl compounds **12** (HO6ONB) and **13** (HO7ONB) was investigated, since the corresponding hydroxy tail terminated 4-alkoxy-4'-cyanobiphenyls (HOnOCB) exhibit stable nematic phase properties [10]. It is observed that compound **12** (HO6ONB) did not show any mesophase property, however compound 1**3** (HO7ONB) exhibits monotropic nematic and smectic phases, and also supercooling properties (see Figure SI) (Figure 3).

The alkoxy nitrobiphenyls (nONB) clearly exhibit an odd-even effect on the transition temperature (clearing point) as the length of the alkyl carbon chain varies. It is noted that lower clearing point was observed for the odd carbon chain compounds 3ONB, 5ONB, and 7ONB compared to even carbon chain compounds 4ONB, 6ONB and 8ONB. However, the clearing point of the fluorine tail terminated alkoxy nitrobiphenyls (FnONB) did not show as clear of an odd-even effect where clearing point goes up initially for F4ONB and then decreases gradually for F5ONB, F6ONB and F7ONB before it increases again for longer chains. As expected, an opposite odd-even effect was observed for alkoxy analogs compared to alkyl analogs, since the oxygen is considered to be sterically equivalent to methylene (-CH_2-) unit [33]. To depict the odd-even effect and compare it in materials with and without terminal tail fluorination, a plot of transition temperature (clearing point) as a function of number of carbons in the alkyl chain is shown in Figure 4.

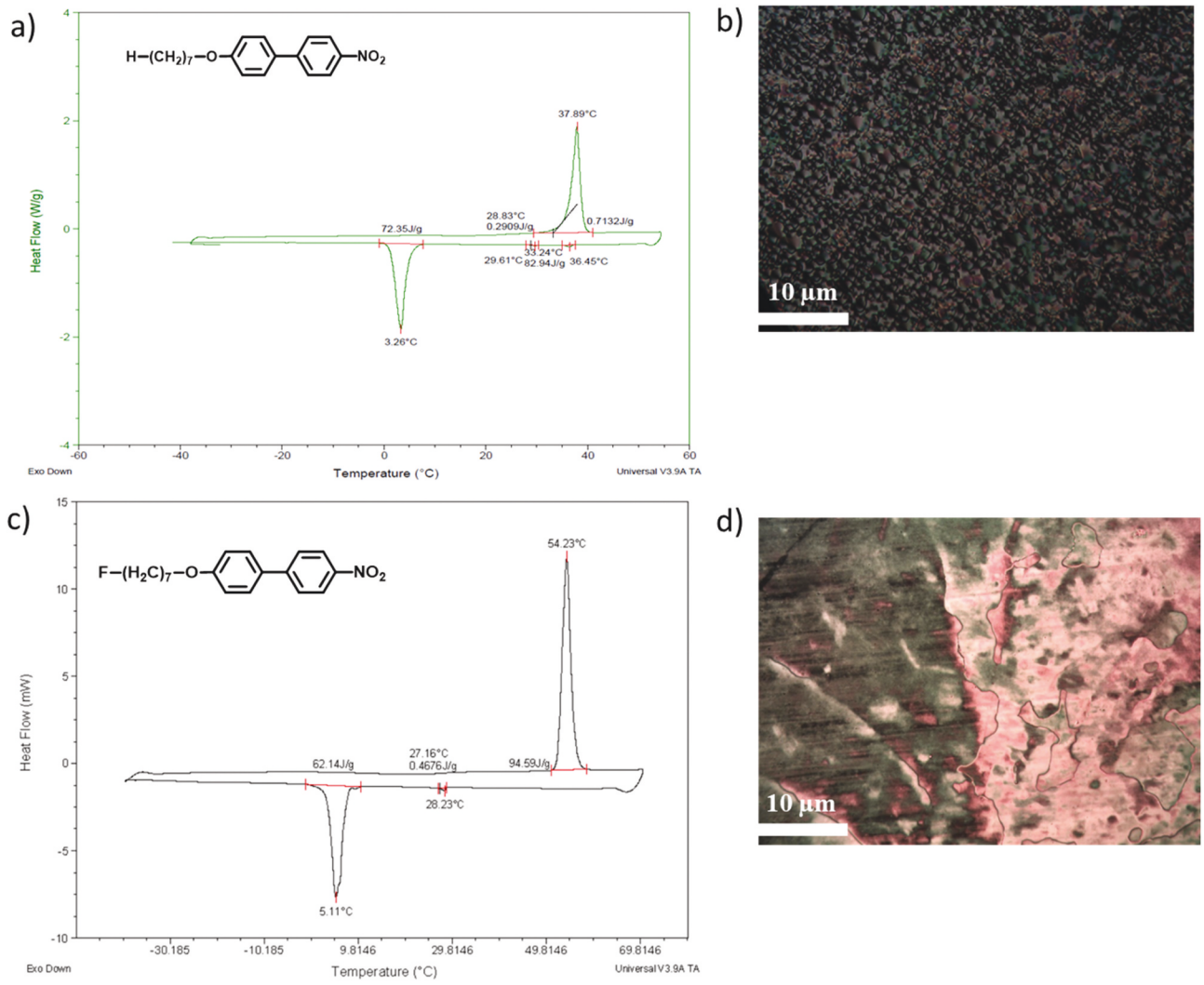

Figure 2. (Colour online) (a) DSC plots of **5e** (K 38.6 I 37.3 N 1.8 K); (b) POM image of **5e** showing nematic texture at 37.2°C on cooling cycle; (c) DSC plot of **10e** (K 54.2 I 28.2 N 5.1 K); and (d) POM image of **10e** showing nematic texture at 28.1°C on cooling cycle.

The phase behaviour data of a smaller set of aromatic core fluorinated 4-alkoxy-4'-nitrobiphenyl compounds **12-13** (nONBF) were analysed by DSC and POM. The POM data of **12, 13** and analogous hydrogen tail terminated 4-alkoxy-4'-nitrobiphenyl compounds **5e** and **5f** is summarised in Table 2.

None of the laterally fluorinated compounds **12-14** exhibit mesogenic behaviour but they do possess supercooling properties. It is also noticed that lateral fluorination to the aromatic core does lower the melting point and clearing points but completely suppresses mesogenic activity compared to the analogous hydrogen tail terminated compounds **5e-g**. For compound **14**, the heating cycle of DSC shows two phase transitions in a very short range from 24°C to 29°C but no phase change was seen in POM analysis. Compound **12** is an isotropic liquid at room temperature but recrystallised at subzero temperature (0.6°C) based on DSC analysis, and therefore, would be suitable for binary mixture analysis to obtain a wider nematic range property.

The dipole moments of the nONB ($n = 3$–10), FnONB ($n = 3$–11), and nONBF ($n = 3$–10) molecules were calculated to better understand how fluorine termination on the alkoxy tail or fluorine substitution on the phenyl ring influences molecular properties. For the nONB and nONBF molecules, the dipole moment is not largely affected by the length of the alkoxy tail. This result is similar to the trend found for the alkyl tail cyanobiphenyl molecules studied previously [10] which also did not have a polar group at the end of the tail of the molecule. Comparison of the dipole moments calculated for the nONB molecules and the nONBF molecules suggests that F-substitution on the phenyl ring increases the dipole moment. The dipole moment of the FnONB molecules increases until $n = 8$, then

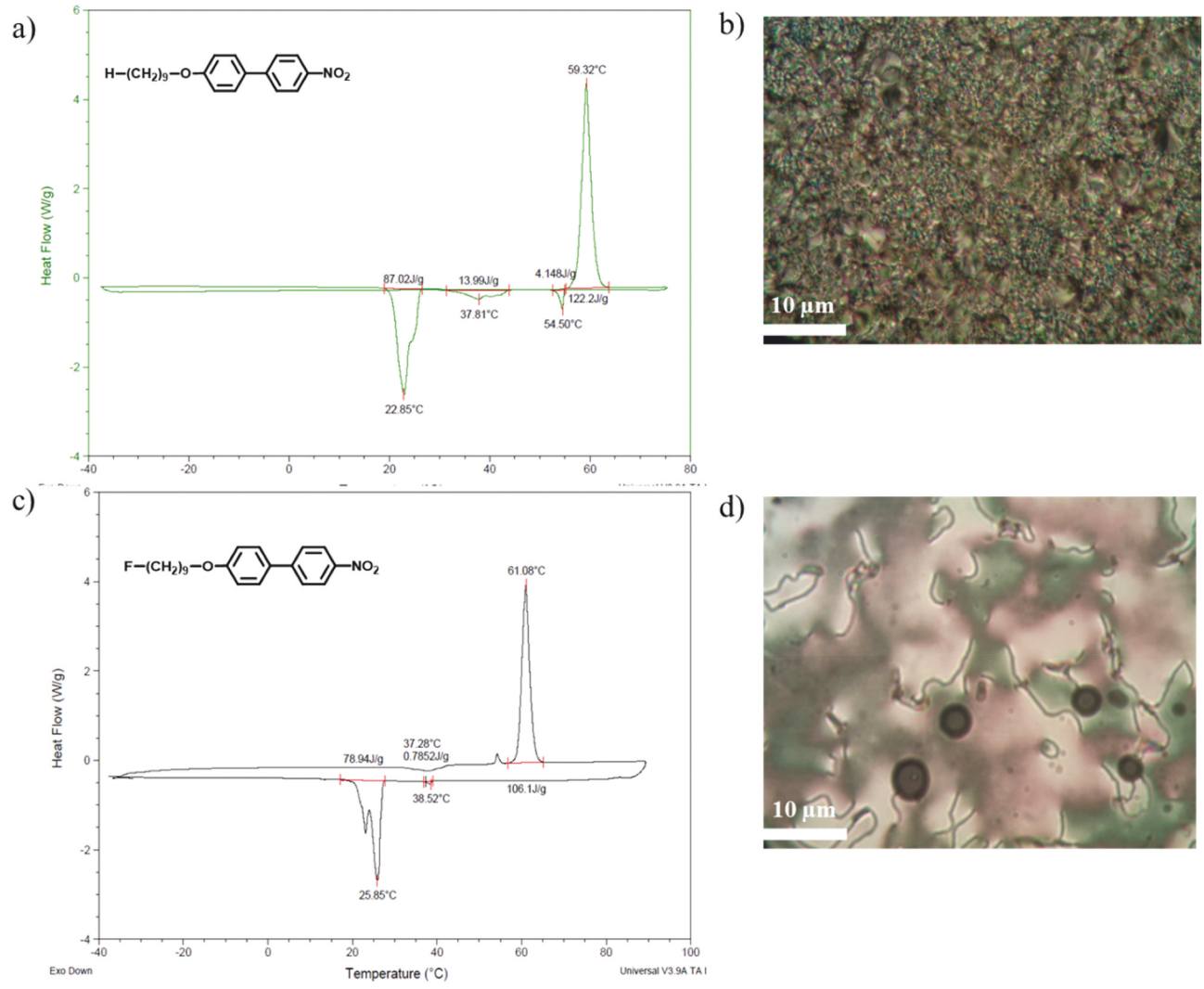

Figure 3. (Colour online) (a) DSC plots of **5g** (K 59.3 I 54.5 Sm 37.8 K1 22.8 K2), (b) POM image of **5g** showing smectic texture at 53.3°C on cooling cycle, (c) DSC plot of **10g** (K 61 I 38.5 N 25.8 K) and (d) POM image of **10g** showing nematic texture at 40.1°C on cooling cycle.

decreases for $n = 9$–11. This occurs because there is a significant number of molecular configurations where the tail has curved around towards the biphenyl core of the molecule. An example configuration with the tail curved back towards the biphenyl nitro group is shown in Figure 5(b).

Figure 6 shows the binding free energy of the LC surrogate molecule $PhNO_2$ to the neutral anion model of five metal salts: $Al(ClO_4)_3$, $Co(ClO_4)_2$, $Cu(ClO_4)_2$, $La(ClO_4)_3$, and $Ni(ClO_4)_2$. $PhNO_2$ serves as a surrogate for both the nONB and FnONB molecules. A calculated negative binding free energy points to a prediction for homeotropic anchoring on that metal salt, while a positive binding free energy points to a prediction for planar anchoring on that metal salt. $Al(ClO_4)_3$ is the only metal salt examined where the binding free energy of $PhNO_2$ is positive. Perfect agreement was found between computational predictions and experimental observations for liquid crystal anchoring on these metal salts.

Figure 7 shows the calculated displacement free energy for DMMP displacing the $PhNO_2$ surrogate molecule of the LC on $Co(ClO_4)_2$, $Cu(ClO_4)_2$, $La(ClO_4)_3$, and $Ni(ClO_4)_2$, which are the metal salts examined that initially have homeotropic anchoring of the liquid crystal. The calculated displacement free energy is between −0.6 eV and −0.8 eV for all four of these metal salts. The displacement free energy has been used as a descriptor for predicting whether displacement will occur for a given LC/surface combination upon exposure to an analyte [31,32]. The hypothesis we have proposed in the past is that there exists a Bronsted-Evans-Polanyi (BEP) correlation between the displacement free energy and the activation free

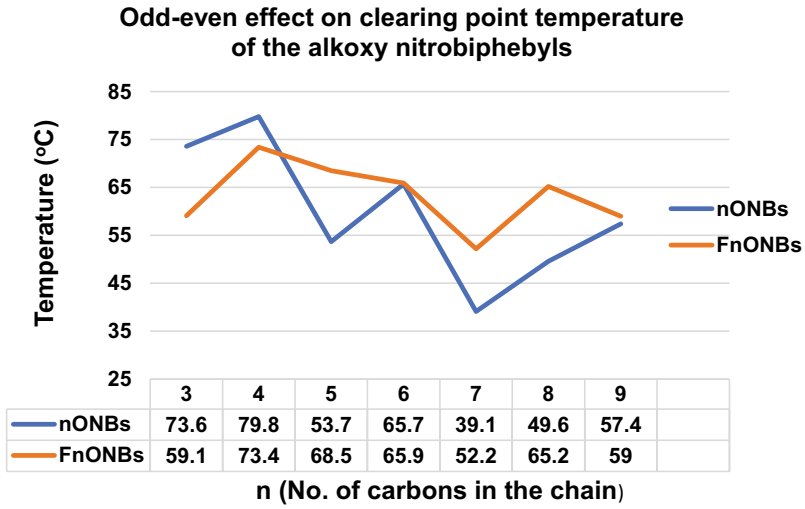

Figure 4. (Colour online) A plot of temperature vs number of carbons in the alkyl chain showing odd-even effect on clearing point of the alkoxy nitrobiphenyl derivatives (nONB and FnONB).

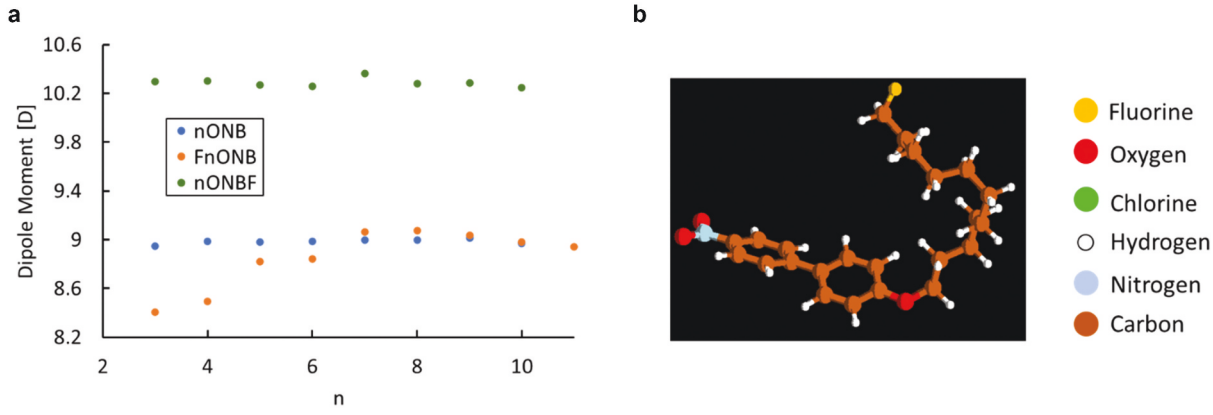

Figure 5. (Colour online) (a) Calculated dipole moment vs. *n* for nONB (blue), and FnONB (orange), and nONBF (green). (b) Example structure of F11ONB with tail turned back toward the biphenyl nitro group.

Table 2. Phase behaviour data of the aromatic core fluorinated 4-alkoxy-4′-nitrobiphenyl compounds 12-14 (nONBF) analysed by POM.

n	nONB	$H(H_2C)_n$–O–⟨⟩–⟨⟩–NO_2	nONBF	$H(H_2C)_n$–O–⟨⟩(F)–⟨⟩–NO_2
7	5e (7ONB)	K 36.3 N 39.1 I 38.9 N 32.6 Sm	12 (7ONBF)	Isotropic (DSC: K 25.4 I 0.6 K)
8	5f (8ONB)	K 48.5 N 49.6 I 49 N 46.3 (Sm) 33.3 K	13 (8ONBF)	K 40.5 I 29.8 K
9	5g (9ONB)	K 57.4 I 53.3 Sm 30.4 K1 27.4 K2	14 (9ONBF)	K 24.8 I

energy barrier for the displacement event [34] so that a more negative displacement energy indicates that the barrier for displacement would be lower and the displacement event more likely. The displacement free energies in Figure 7 indicate that displacement of the LC molecule by DMMP is exergonic, and, using thresholds developed in past studies, we conclude that the magnitude of the displacement free energies would predict displacement [31,32]. Yet, displacement of the LC by DMMP is not experimentally observed on any of the four salts studied. We hypothesise that the barrier to displacement is larger for this LC molecule than for 5CB

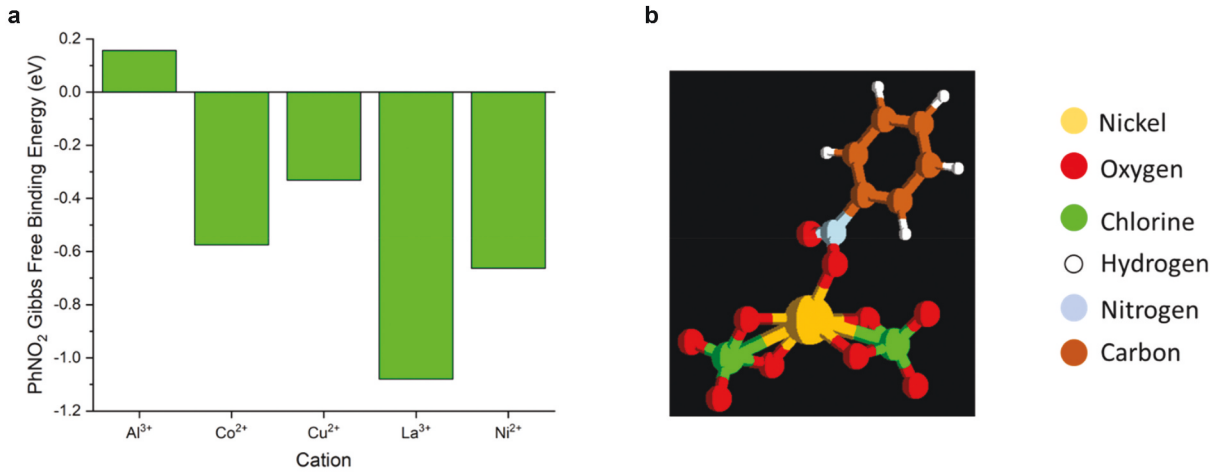

Figure 6. (Colour online) (a) Calculated binding free energy for $PhNO_2$ adsorption on $Al(ClO_4)_3$, $Co(ClO_4)_2$, $Cu(ClO_4)_2$, $La(ClO_4)_3$, and $Ni(ClO_4)_2$. A positive binding free energy suggests planar anchoring, while a negative binding free energy suggests homeotropic anchoring. (b) Energy-minimized structure for $PhNO_2$ bound to the neutral anion model of $Ni(ClO_4)_2$.

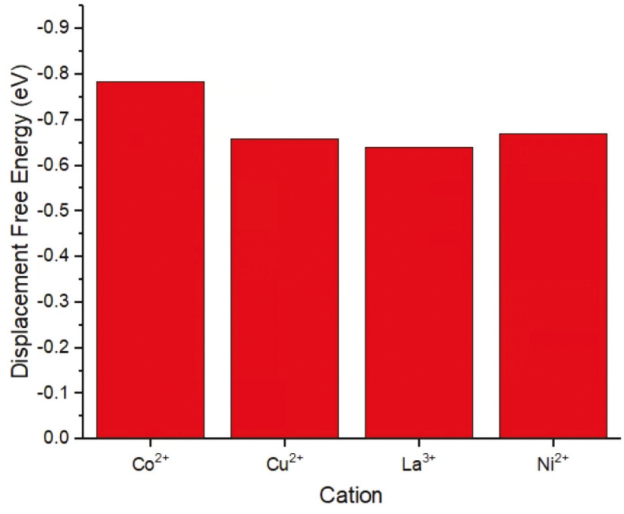

Figure 7. Calculated displacement free energy of DMMP displacing $PhNO_2$ on $Co(ClO_4)_2$, $Cu(ClO_4)_2$, $La(ClO_4)_3$, and $Ni(ClO_4)_2$. No displacement is experimentally observed upon exposure to DMMP on any of these four salts.

used previously, and the displacement free energy would therefore need to be even more negative for an experimentally observable response. In other words, this disagreement between theory and experiment points to significant kinetic limitations for the displacement event, not accounted for in the present study.

We performed experiments using LC cells composed of two identically prepared metal salt-decorated surfaces to eliminate the confounding influence of the LC-air interface on the orientation of the LC. The experimental methods in this section can be found in our previous work [32]. Consistent with the computational predictions of negative binding free energy values of $PhNO_2$ binding on $Co(ClO_4)_2$, $Cu(ClO_4)_2$, $La(ClO_4)_2$, $Ni(ClO_4)_2$, we observed homeotropic ordering of 7ONB on surfaces decorated with metal salts (Figure 8(a)). We also observed that for a surface decorated with $Al(CLO_4)_3$, 7ONB exhibits a planar ordering which is consistent with a positive binding free energy of $PhNO_2$ to the surface.

We also studied the response of 7ONB to 1300 ppm ozone gas. Previous studies indicate that ozone can oxidise metal salt surfaces and form metal oxide [35]. Weak binding free energy of LC mesogen to the metal oxide surface has been reported in agreement with an experimentally observed planar anchoring. We performed experiments with 7ONB supported on 15 pmol mm^{-2} $Ni(ClO_4)_2$, $Co(ClO_4)_2$ and $Cu(ClO_4)_2$ surfaces and observed an anchoring transition to planar within a minute of ozone exposure as indicated in Figure 9. This is consistent with observations in previous studies where the oxidation of metal salt surfaces is reported by an anchoring transition in the LC.

3. Conclusions

A novel series of fluorine tail terminated 4-alkoxy-4'-nitrobipheny compounds (FnONB) and lateral fluorine substituted 4-alkoxy-4'-nitrobipheny compounds (nONBF) have been developed. In this work, we also reported the synthesis of analogous hydrogen tail terminated 4-alkoxy-4'-nitrobipheny compounds (nONB) applying a modified synthetic procedure. The phase behaviour of the fluorine tail terminated, and lateral fluorine substituted 4-alkoxy-4'-nitrobipheny compounds were investigated and compared with the analogous hydrogen tail terminated 4-alkoxy-4'-nitrobipheny

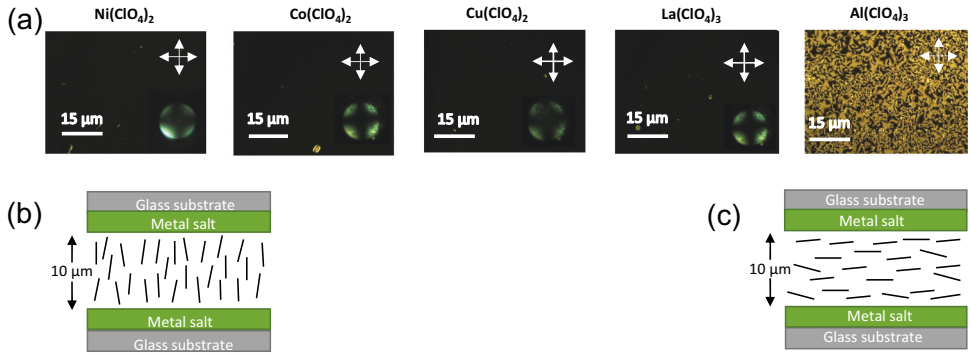

Figure 8. (Colour online) (a) Cross-polarized images of 7ONB confined between two glass surfaces decorated with different metal salt coating of surface density ∽50 pmol/mm^2 at $T = 37.5$°C. (b) Schematic illustration of experimental setup and director profile of 7ONB when it adopts homeotropic orientation (b) and planar orientation (c) respectively on metal salts.

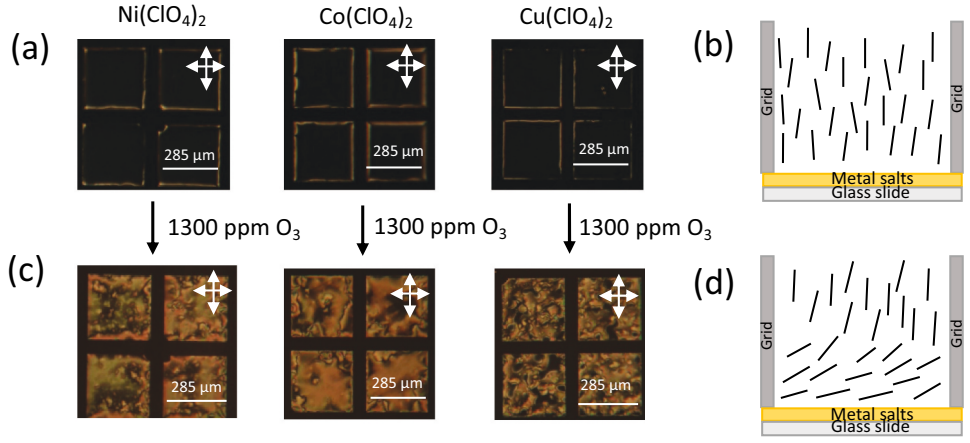

Figure 9. (Colour online) Cross-polarized images of 7ONB on glass slides coated with 15 pmol mm^{-2}metal salts before(a) and after(c) 1300 ppm ozone exposure; (b), (d) schematic illustration of the experimental setup and LC director profile.

compounds. While some the fluorine tail functionalised compounds exhibited nematic behaviour, they did not show improved mesophase behaviour for F3ONB, F4ONB, F5ONB and F6ONB compared to their non-fluorinated counterparts. Unlike the mesogenic behaviour (enantiotropic nematic and monotropic smectic phase transition) of 7ONB and 8ONB, the fluorine tail terminated compounds F7ONB and F8ONB show monotropic nematic phase and supercooling properties. Furthermore, fluorine tail termination suppresses the smectic phase transition that was observed for the longer chain hydrogen tail compounds (7ONB-10ONB). Interestingly, phase behaviour for both 7ONB and 8ONB in our analysis demonstrates an enantiotropic nematic phase and monotropic smectic phase transitions, whereas monotropic nematic and smectic phase transitions for 7ONB, and enantiotropic nematic and smectic phase transitions for 8ONB were reported. On the other hand, no improvement but rather the complete destabilisation of mesogenic properties was observed for the lateral fluorine substituted compounds (7-8ONBF) compared to the analogous hydrogen and fluorinated tail compounds (7-8ONB and F7-8ONB). Moreover, fluorine tail terminated compound F7ONB shows a broad nematic phase property till subzero range, and therefore, it could potentially be a useful compound for chemoresponsive sensors. The study of the chemoresponsive properties and applications of these fluorinated and non-fluorinated materials is underway.

Disclosure statement

Prof. Nicholas L. Abbott declares a financial interest in Platypus Technologies LLC, a for-profit company that has developed LC-based analytic technologies for conflicts of interest.

Funding

This work was supported by three grants from the National Science Foundation (DMR-1921696, DMR-1921722, and DMR-1921668). Part of the computational work conducted by T.W. and M.M. in this study was carried out through

external computational resource facilities at the National Energy Research Scientific Computing Centre (NERSC) through the U.S. DOE, Office of Science under Contract No. DE-AC02-05CH11231; and the Centre for Nanoscale Materials (CNM) at Argonne National Laboratory (ANL) through the U.S. DOE, Office of Science under Contract No. DE-AC02-06CH11357.

References

[1] Gray GW. Synthetic chemistry related to liquid-crystals. Mol Cryst Liq. 1973;21(1–2):161–186.
[2] Shah RR, Abbott NL. Principles for measurement of chemical exposure based on recognition-driven anchoring transitions in liquid crystals. Science. 2001;293(5533):1296–1299.
[3] Nayani K, Rai P, Bao NQ, et al. Liquid crystals with interfacial ordering that enhances responsiveness to chemical targets. Adv Mater. 2018;30(27):7. DOI:10.1002/adma.201706707
[4] Szilvási T, Bao N, Nayani K, et al. Redox-triggered orientational responses of liquid crystals to chlorine gas. Angew Chem. 2018;130(31):9813–9817. DOI:10.1002/ange.201803194
[5] Gray GW, Harrison KJ, Nash JA. New family of nematic liquid-crystals for displays. Electron Lett. 1973;9(6):130–131.
[6] Luo ZY, Peng FL, Chen HW, et al. Fast-response liquid crystals for high image quality wearable displays. Opt Mater Express. 2015;5(3):603–610. DOI:10.1364/OME.5.000603
[7] Geelhaar T, Griesar K, Reckmann B. 125 years of liquid crystals—a scientific revolution in the home. Angew Chem Int Ed Engl. 2013;52(34):8798–8809.
[8] Itahara T. Effect of the pentafluorophenyloxy group on liquid crystalline behaviour. Liq Cryst. 2005;32(1):115–118.
[9] Wang KL, Szilvasi T, Gold J, et al. New room temperature nematogens by cyano tail termination of alkoxy and alkylcyanobiphenyls and their anchoring behavior on metal salt-decorated surface. Liq Cryst. 2020;47(4):540–556. DOI:10.1080/02678292.2019.1662116
[10] Wang K, Jirka M, Rai P, et al. Synthesis and properties of hydroxy tail-terminated cyanobiphenyl liquid crystals. Liq Cryst. 2019;46(3):397–407. DOI:10.1080/02678292.2018.1502373
[11] Wang K, Rai P, Fernando A, et al. Synthesis and properties of fluorine tail-terminated cyanobiphenyls and terphenyls for chemoresponsive liquid crystals. Liq Cryst. 2020;47(1):3–16. DOI:10.1080/02678292.2019.1616228
[12] Wang KL, Rahman MS, Szilvasi T, et al. Influence of multifluorophenyloxy terminus on the mesomorphism of the alkoxy and alkyl cyanobiphenyl compounds in search of new ambient nematic liquid crystals and mixtures. Liq Cryst. 2021;48(5):672–688. DOI:10.1080/02678292.2020.1810792
[13] Rupar I, Mulligan KM, Roberts JC, et al. Elucidating the smectic a-promoting effect of halogen end-groups in calamitic liquid crystals. J Mater Chem C. 2013;1(23):3729–3735. DOI:10.1039/c3tc30534a
[14] Davis EJ, Mandle RJ, Russell BK, et al. Liquid-crystalline structure-property relationships in halogen-terminated derivatives of cyanobiphenyl. Liq Cryst. 2014;41(11):1635–1646. DOI:10.1080/02678292.2014.940505
[15] Gibb CJ, Storey JMD, Imrie CT. A convenient one-pot synthesis, and characterisation of the ω-bromo -1-(4-cyanobiphenyl-4'-yl) alkanes (CBnBr). Liq Cryst. 2022;1–11. DOI:10.1080/02678292.2022.2084568
[16] Kumar S, Pal SK. The first examples of terminally thiol-functionalized alkoxycyanobiphenyls. Liq Cryst. 2005;32(5):659–661.
[17] Zhu SB, Jin CG, Li W, et al. The effect of intermolecular actions on the mesomorphic properties of alkenoxy biphenyl-based liquid crystals. J Mol Liq. 2019;296:8.
[18] Mandle RJ, Cowling SJ, Sage I, et al. Relationship between molecular association and re-entrant phenomena in polar calamitic liquid crystals. J Phys Chem B. 2015;119(7):3273–3280. DOI:10.1021/jp512093j
[19] Mandle RJ, Cowling SJ, Goodby JW. Evaluation of 4-alkoxy-4 '-nitrobiphenyl liquid crystals for use in next generation scattering LCDs. RSC Adv. 2017;7(64):40480–40485.
[20] Zugenmaier P, Kuczynski W. Comparison of the crystal and molecular structures of three similar 4-heptylbiphenyl compounds: 4-heptyl-4′-cyanobiphenyl, 4-heptyl-3′-cyanobiphenyl, and 4-heptyl-4′-nitrobiphenyl. Mol Cryst Liq Cryst. 2006;457(1):93–103.
[21] Yamada S, Rokusha Y, Kawano R, et al. Mesogenic gold complexes showing aggregation-induced enhancement of phosphorescence in both crystalline and liquid-crystalline phases. Faraday Discuss. 2017;196:269–283.
[22] Jones B, Chapman F. 337. The nitration of esters of 4-hydroxydiphenyl. The preparation of 4-hydroxy-4′-and-2′-nitrodiphenyls. J Chem Soc. 1952;1829–1832. DOI:10.1039/JR9520001829
[23] Ding R, He Y, Wang X, et al. Treatment of alcohols with tosyl chloride does not always lead to the formation of tosylates. Molecules. 2011;16(7):5665–5673. DOI:10.3390/molecules16075665
[24] Kabalka GW, Varma M, Varma RS, et al. Tosylation of alcohols. J Org Chem. 1986;51(12):2386–2388. DOI:10.1021/jo00362a044
[25] Frisch M, Trucks G, Schlegel HB, et al. Gaussian 09, revision d. 01, gaussian. Wallingford CT: Inc; 2009. p. 201.
[26] Perdew JP, Burke K, Ernzerhof M. Generalized gradient approximation made simple (vol 77, pg 3865, 1996). Phys Rev Lett. 1997;78(7):1396.
[27] Grimme S, Antony J, Ehrlich S, et al. A consistent and accurate ab initio parametrization of density functional dispersion correction (DFT-D) for the 94 elements H-Pu. J Chem Phys. 2010;132(15):19. DOI:10.1063/1.3382344
[28] Marenich AV, Cramer CJ, Truhlar DG. Universal solvation model based on solute electron density and on a continuum model of the solvent defined by the bulk dielectric constant and atomic surface tensions. J Phys Chem B. 2009;113(18):6378–6396.

[29] Weigend F, Ahlrichs R. Balanced basis sets of split valence, triple zeta valence and quadruple zeta valence quality for H to Rn: design and assessment of accuracy. Phys Chem Chem Phys. 2005;7(18):3297–3305.
[30] Zhao Y, Truhlar DG. The M06 suite of density functionals for main group thermochemistry, thermochemical kinetics, noncovalent interactions, excited states, and transition elements: two new functionals and systematic testing of four m06-class functionals and 12 other functionals. Theor Chem Acc. 2008;120(1–3):215–241.
[31] Yu HZ, Szilvasi T, Rai P, et al. Computational chemistry-guided design of selective chemoresponsive liquid crystals using pyridine and pyrimidine functional groups. Adv Funct Mater. 2018;28(13):10. DOI:10.1002/adfm.201703581
[32] Szilvasi T, Bao NQ, Yu HZ, et al. The role of anions in adsorbate-induced anchoring transitions of liquid crystals on surfaces with discrete cation binding sites. Soft Matter. 2018;14(5):797–805. DOI:10.1039/C7SM01981E
[33] Collings PJ, and Hird M. Introduction to liquid crystals chemistry and physics. London: CRC Press; 2017.
[34] Roling LT, Scaranto J, Herron JA, et al. Towards first-principles molecular design of liquid crystal-based chemoresponsive systems. Nat Commun. 2016;7(1):7. DOI:10.1038/ncomms13338
[35] Bao NQ, Gold JI, Szilvasi T, et al. Designing chemically selective liquid crystalline materials that respond to oxidizing gases. J Mater Chem C. 2021;9(20):6507–6517. DOI:10.1039/D1TC00544H